

## Supporting Information

for

### **2,2'-bipyridine Zn(II) complexes: role of the 4,4' substituents on the crystalline solid state properties**

*Yogesh J. Yadav, Teresa F. Mastropietro, Elisabeta Ildyko Szerb, Anna Maria Talarico, Sante Pirillo, Daniela Pucci, Alessandra Crispini and Mauro Ghedini*

**Figure S1.** NMR spectra of the free ligand L1 (a) and the adduct **1a**  $\{[(\text{L1})_3\text{Zn}](\text{PF}_6)_2\}_2 \cdot \text{L1} \cdot 2\text{H}_2\text{O}$  (b) with the proton of the coordinated bipyridines labeled as  $_{\text{Zn}}\text{H}^3$ ,  $_{\text{Zn}}\text{H}^5$  and  $_{\text{Zn}}\text{H}^6$ .

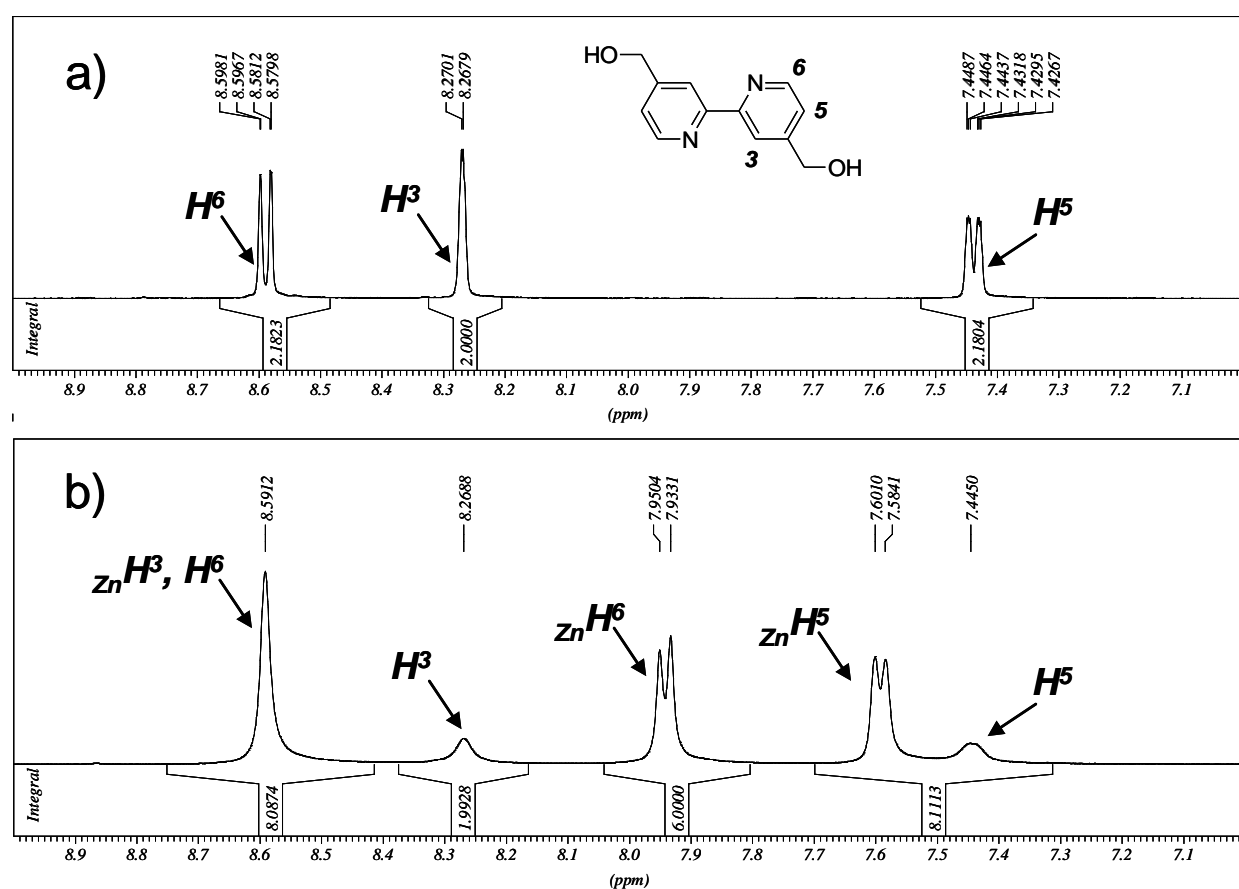


**Figure S2.** PXRD spectrum of the reaction product after grinding in the synthesis of **2a** (black line) superimposed to that of **2** (red line)

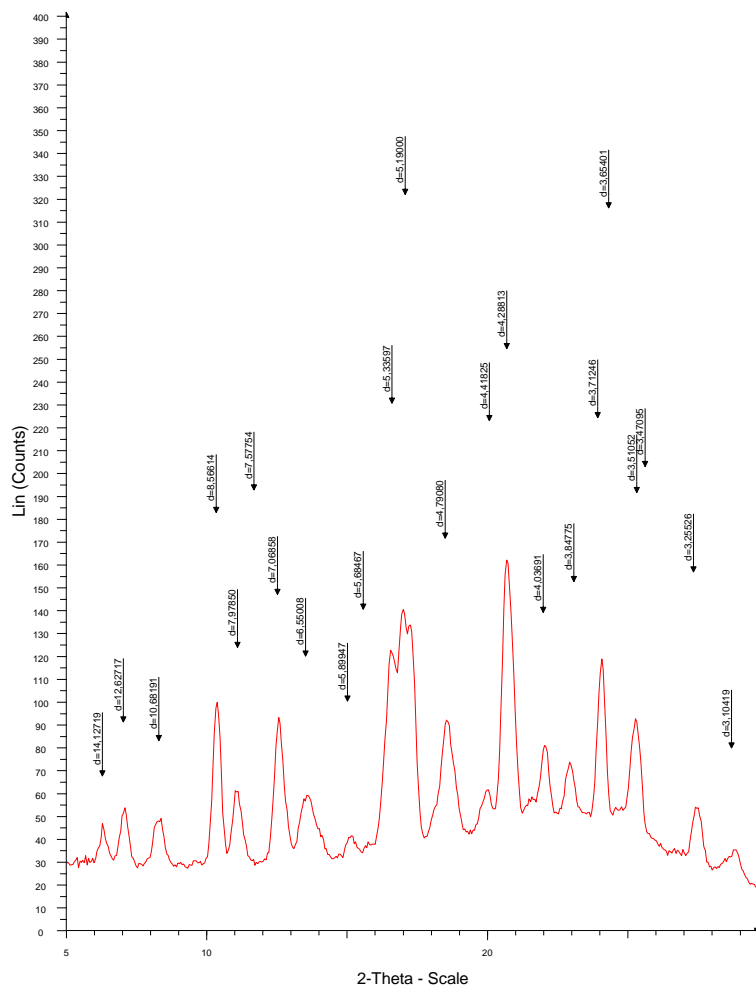


**Figure S3.** PXRD spectrum of the reaction product after grinding in the synthesis of **2b** (black line) superimposed to that of **2** (red line)

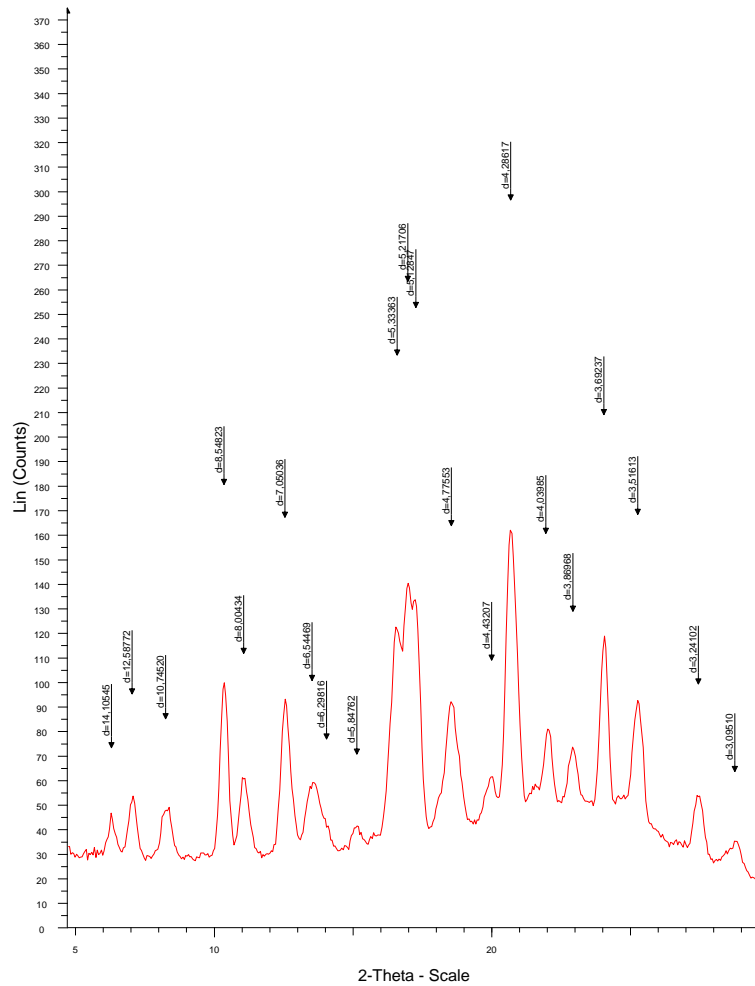


**Figure S4.** Crystals of the supramolecular adduct **2a** (a) and precursor **2** (b).

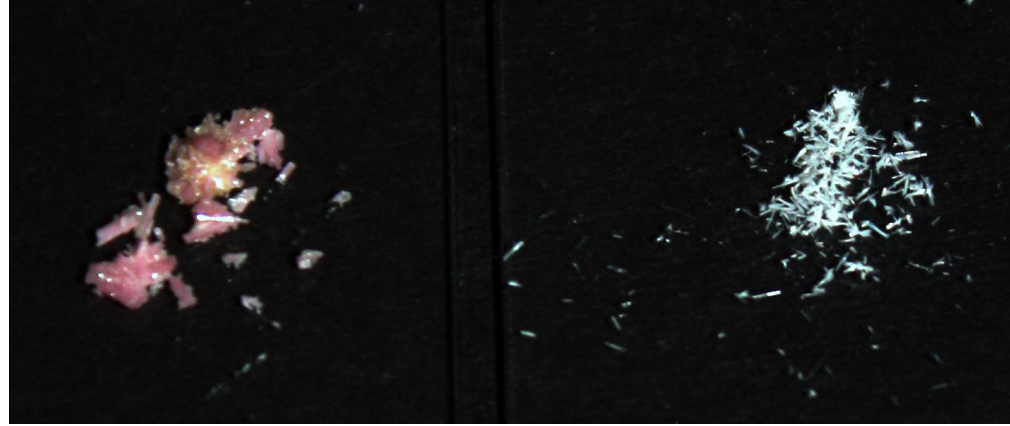
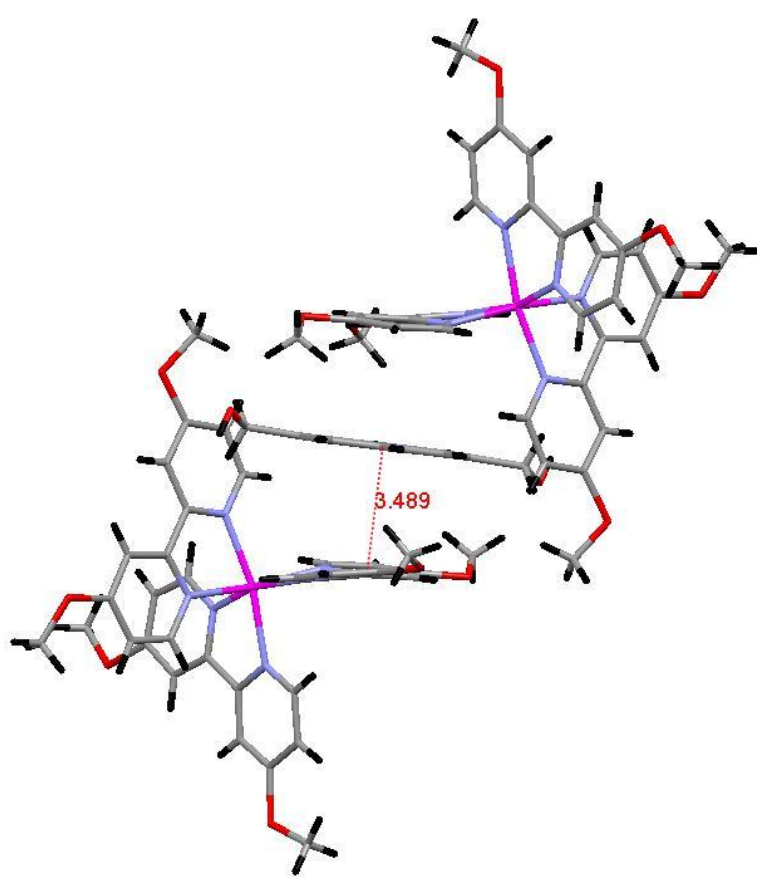


**Table S1** Details of data collection and structure refinements for complexes **1a**, **2a** and **2**

	<b>1a</b>	<b>2a</b>	<b>2</b>	<b>L<sub>1</sub></b>
formula	C <sub>84</sub> H <sub>88</sub> F <sub>24</sub> N <sub>14</sub> O <sub>16</sub> P <sub>4</sub> Zn <sub>2</sub>	C <sub>84</sub> H <sub>88</sub> F <sub>24</sub> N <sub>14</sub> O <sub>16</sub> P <sub>4</sub> Zn <sub>2</sub>	C <sub>36</sub> H <sub>36</sub> F <sub>12</sub> N <sub>6</sub> O <sub>6</sub> P <sub>2</sub> Zn	C <sub>12</sub> H <sub>12</sub> N <sub>2</sub> O <sub>2</sub>
<i>M<sub>r</sub></i>	2260.30	2260.30	1004.02	216.24
crystal system	Triclinic	Triclinic	Triclinic	Monoclinic
space group	<i>P</i> - <i>I</i>	<i>P</i> - <i>I</i>	<i>P</i> - <i>I</i>	<i>p</i> (2) <i>I</i> / <i>c</i>
<i>a</i> [Å]	12.0842(18)	12.1158(12)	11.354(3)	7.507(5)
<i>b</i> [Å]	14.630(2)	14.8243(18)	13.202(4)	12.063(8)
<i>c</i> [Å]	14.997(2)	15.0480(17)	15.056(5)	16.970(11)
$\alpha$ [°]	68.239(7)	67.610(5)	76.794(13)	90
$\beta$ [°]	88.188(7)	87.958(5)	76.652(13)	96.79(2)
$\gamma$ [°]	76.637(7)	76.494(5)	83.772(13)	90
<i>V</i> [Å <sup>3</sup> ]	2391.4(6)	2425.6(5)	2134.0(12)	1526.0(18)
<i>Z</i>	1	1	2	6
$\rho$ cald [gcm <sup>-3</sup> ]	1.569		1.563	1.412
$\mu$ [cm <sup>-1</sup> ]	0.686		0.754	0.098
$\theta$ range [°]	1.46-26.33		1.42-26.15	2.08 to 25.02°
data collected	103631		69588	15114
unique data, <i>R</i> <sub>int</sub>	9640, 0.0599		8353, 0.0414	2649, 0.0552
obs. data	6787		6545	2649
[ <i>I</i> > 2 $\sigma$ ( <i>I</i> )]			568	220
no. parameters	647		0.0457	0.0485
<i>R</i> <sub>f</sub> [obs. data]	0.0873		0.1394	0.1244
<i>wR</i> <sub>2</sub> [all data]	0.2660		1.019	1.024
GOF	1.186			

**Figure S5** View of the supramolecular tetra-cationic complex supported by  $\pi$ - $\pi$  stacking in **2a**.



### Structural description of L<sub>1</sub>.

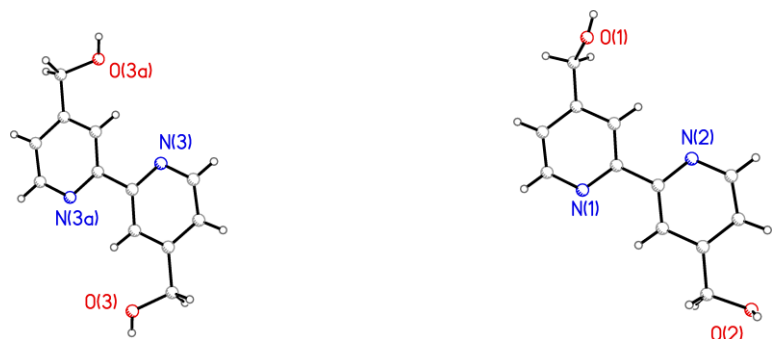


**Figure S6** View of the L<sub>1</sub> ligand showing the atomic labelling scheme;  $a = (x-1, 1-y, -z)$

The crystal structure of the pure ligand L<sub>1</sub> is made up of two crystallographic non equivalent ligands, one of them lying on an inversion centre, both showing the usual NN *trans* conformation. The heteroaromatic rings of the ligands assemble into a columnar organization by means of  $\pi \cdots \pi$  stacking interactions [shortest distances between pyridine planes in the range of 3.4-3.5 Å, as provided by PLATON analysis]. The shortest interplanar distances are observed between pairs of  $\pi \cdots \pi$  stacked ligands for which the additional contribution of hydrogen bonding interactions, similar to those observed in **1a**, is present (Figure 3) [O(2)…O(1)<sup>*i*</sup> 2.76(1); O(2)-H(2a)…O(1)<sup>*i*</sup> distance and angle of 1.952 Å and 167.32° respectively;  $i = -x+1, -y, -z+2$ ], proving the tendency of hydrogen bonds to support stacking interactions in these systems.

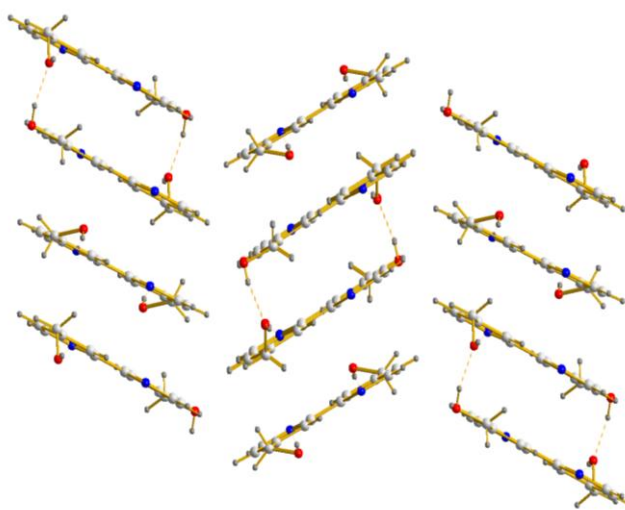


**Figure S7** View of the supramolecular packing along the  $a$  crystallographic axis in L<sub>1</sub>.